https://doi.org/10.5194/egusphere-2025-3756
Preprint. Discussion started: 12 September 2025

Predictability of mean summertime diurnal winds over ungauged mountain glaciers

J Krishnanand[1], Argha Banerjee[1], R. Shankar[2], Himanshu Kaushik[3], Mohd. Farooq Azam[3], and Chandan Sarangi[4]

[1]Earth and Climate Science, Indian Institute of Science Education and Research Pune, Maharashtra, India
[2]The Institute of Mathematical Sciences, Chennai, Tamil Nadu, India
[3]Department of Civil Engineering, Indian Institute of Technology Indore, Madhya Pradesh, India
[4]Department of Civil Engineering, Indian Institute of Technology Madras, Tamil Nadu, India

Correspondence: Argha Banerjee (argha@iiserpune.ac.in)

Abstract. Glacier and valley winds are typical characteristics of the microclimate of glacierised valleys. The speed of such winds determines the turbulent heat flux, which contributes to ice melt. Sparse in-situ meteorological measurements and the inability of large-scale climate data products to capture such local winds introduce uncertainty into glacier- to global-scale mass-balance calculations. Here, we propose an empirical model having three parameters, namely, the mean wind speed, the sensitivity of the diurnal winds to temperature, and a response time, to predict the mean summertime diurnal wind speed on valley glaciers based only on reanalysis temperature. Utilising data from 28 weather stations on 18 valley glaciers across the globe, we show that the model reproduces the observed mean summertime diurnal wind speed reasonably well. Furthermore, we show that the three model parameters can be estimated at any glacier using a few topographic variables, allowing prediction of wind speed on ungauged glaciers. A leave-one-out analysis of the stations suggests a root-mean-squared error of 0.76 ms^{-1} on average, which is a ∼300% improvement over a standard reanalysis product. The performance of the model is largely independent of the number of stations available for calibration, as long as it is 20 or more. More work is needed to explain the physical mechanisms underlying the predictability of the mean diurnal wind speed on ungauged glaciers based solely on reanalysis temperature and a few topographic variables. The presented model can improve wind speed estimates on ungauged glaciers, leading to better glacier mass-balance calculations at various spatial scales.

1 Introduction

The microclimate of a glacierised valley has a characteristic system of local winds consisting of a glacier wind and a valley wind (e.g., Oerlemans, 2010). Glacier wind is a shallow (of the order of $\sim 10^1$ m), persistent, katabatic wind flowing down-valley, consisting of air cooled by the ice surface acted upon by a down-slope buoyancy forcing (Oerlemans, 2010). Away from the glacier, as the valley floor and the hillsides are heated up during the day by solar insolation, the buoyancy forcing acts up-slope, leading to a daytime up-valley valley wind that is relatively deeper (of the order of $\sim 10^2$ m) (Nickus and Vergeiner, 1984; Vergeiner and Dreiseitl, 1987; Broeke, 1997a, b). Near the glacier termini, glacier and valley winds compete with each other at the surface level during the day (e.g., Cai et al., 2007). The buoyancy forcing in the valley, and consequently the

https://doi.org/10.5194/egusphere-2025-3756
Preprint. Discussion started: 12 September 2025

valley wind, changes sign at night (e.g., Mannouji, 1982). This leads to a diurnal cycle of valley winds with up-valley (down-valley) flow during the day (night). Both of these winds fall under the general category of thermally driven slope winds (Farina and Zardi, 2023), which can be described approximately using the steady-state Prandtl model (Prandtl, 1952). This model describes the vertical profile of slope winds via a dynamic equilibrium between buoyant force and friction, and reproduces the characteristic wind speed maxima or jet at a height of a few meters above the surface (e.g., Oerlemans, 2010). With a thermodynamic approach to the problem, a simple energy exchange model was also successfully used to describe the effect of katabatic cooling due to glacier wind on the variation of 2m-air temperature along the flow-line of glaciers (Greuell and Böhm, 1998; Ayala et al., 2015). During the ablation season, a linear relation between instantaneous glacier wind speed and ambient air temperature has been empirically observed (e.g., Björnsson et al., 2005). Similar trends have also been reported for valley winds (e.g., Mannouji, 1982). This may imply that the buoyancy forces scale with the horizontal temperature gradient between the valley and the surrounding terrain (Miller et al., 2003).

Accurate knowledge of instantaneous wind speed on glaciers is important for energy- and mass-balance studies, as surface winds mediate energy and mass exchanges between the atmosphere and glacier surface (Cuffey and Paterson, 2010; Stigter et al., 2018). For example, the latent heat fluxes due to these winds determine sublimation rates of snow, which can cause up to $\sim$ 10–90% of the total glacier melt (e.g., Yáñez San Francisco et al., 2025; Stigter et al., 2018; Mandal et al., 2022), and are the dominant source of ablation for high-altitude glaciers in arid regions (Mandal et al., 2022). The net turbulent heat fluxes due to these winds can cause up to $\sim$ 10–35% of the total melt on some glaciers in the Himalaya (e.g., Azam et al., 2014), the Alps (e.g., Oerlemans et al., 1999), and Alaska (e.g., Klok et al., 2005). The turbulent fluxes are also important in the context of the climate response of glaciers. This is because the response of glaciers to the temperature change is largely determined by the corresponding changes in the long-wave radiation balance and those in the turbulent heat fluxes (Oerlemans, 2001). The near-surface lapse rate on a glacier surface varies depending on the presence of glacier or valley winds (Shea and Moore, 2010), which has important consequences for the accuracy of the glacier melt as estimated using simple temperature-index models (Hock, 1999, 2003). The presence of extensive supra-glacial debris cover favours valley winds over the ablation zone (Collier et al., 2015), which also influences the glacier energy balance and the moisture transport along the valley (Lin et al., 2021).

The above discussion highlights the importance of accurate wind speed estimates for glacier energy- and mass-balance studies. However, the number of glaciers where in-situ meteorological measurements are (publicly) available is probably of the order of $\sim 10^2$ or less. This means a majority of $\sim 2.75 \times 10^5$ glaciers on earth are ungauged. On these glaciers, coarse-scale reanalysis wind-speed products need to be used to estimate turbulent heat fluxes (e.g., Rupper and Roe, 2008; Rye et al., 2010). Even on the small minority of the glaciers, where weather stations are present, the data are often available for a relatively short period, or have gaps. On such glaciers, coarse-scale reanalysis data (e.g., Arndt et al., 2021; Kronenberg et al., 2022) have to be used in conjunction with the weather station data. The coarse $\gtrsim$10-km resolution reanalysis products do not capture local-scale winds, and heavily underestimate their speed, and therefore, the associated turbulent fluxes (Draeger et al., 2024). The reanalysis temperature estimates on the other hand, owing to a longer spatial correlation length, are relatively more accurate (Draeger et al., 2024). Various down-scaling methods are typically applied to these coarse-scale wind-speed

https://doi.org/10.5194/egusphere-2025-3756
Preprint. Discussion started: 12 September 2025

products to estimate the local-scale winds. Statistical down-scaling models (Dujardin and Lehning, 2022; Hu et al., 2023), which essentially fit coarse-resolution climate products to point-scale weather-station data, do not work well on data-scarce mountain glaciers. Physically based methods (e.g., Burlando et al., 2007) that rely on simple scaling relations between local and large-scale climate variables cannot be applied on glacierised valleys as they do not incorporate the microclimatic effects of glaciers. Dynamical down-scaling (Goger et al., 2022; Draeger et al., 2024; Tiwari and Bush, 2025) requires high-resolution regional climate model simulations, which are computationally intensive and are impractical for regional- to global-scale studies. Thus, there is a clear need for a simple physically-based model of wind speed on glaciers that can be applied to ungauged mountain glaciers globally.

This study proposes a simple model to estimate the mean diurnal cycle of wind speed during summer on any glacier, solely based on easy-to-access reanalysis temperature and topographic data. In-situ data from a set of 28 on- or near-glacier weather stations worldwide are used to calibrate the model. We evaluate the predictive power of this model on an ungauged glacier using a leave-one-out analysis, and also assess its performance as a function of the number of stations used for calibration. We discuss the limits of applicability of the model and its potential utility for ungauged glaciers.

2 Data

2.1 Automatic weather stations

The hourly time series of wind speed and wind direction observed at 28 weather stations (Fig. 1a) were used in this study. The data were primarily sourced from open-access online databases Zenodo and Pangaea, along with a few other publicly available datasets from the literature (Supplementary Table S1). Since we were interested in on- or near-glacier winds, a spatial filter was applied to select the stations within a 1 km buffer around any glacier (Fig. 1b). Only stations with more than 8 weeks of data during the summer months were used. For glaciers located in the northern (southern) hemisphere, the summer was assumed to be 1st June to 30th September (1st December to 31st March).

This procedure yielded 28 weather stations located on or near 18 glaciers with an approximately global coverage (Fig. 1a), though the southern hemisphere was under-represented. There were 14 stations from the Himalaya, 6 from the Canadian Rockies, 5 from the European Alps, and one each from Alaska, the Caucasus, and the Southern Andes. Out of the 28 stations, 27 were within latitudes of 28°–80°N, and only one station was in the southern hemisphere. The elevation of the stations ranged from 196 m to 8323 m above sea level. The available stations sampled a wide variety of mountain glaciers, with their lengths being in the range 2–45 km and the widths in the range 0.3–14.2 km. Six of the glaciers were debris-covered ones, and the remaining 12 were clean glaciers (Supplementary Table S1). The number of days for which data were available ranged between 56–586, with a median of 198. For the 28 weather stations, the hourly time-series of 2-m wind speed for the summer months were selected for all the available years (see Fig. 2a for an example). The mean summertime diurnal wind speed at a station was calculated by averaging wind speeds for each hour of the day for the entire duration of the dataset (Fig. 2b).

https://doi.org/10.5194/egusphere-2025-3756
Preprint. Discussion started: 12 September 2025

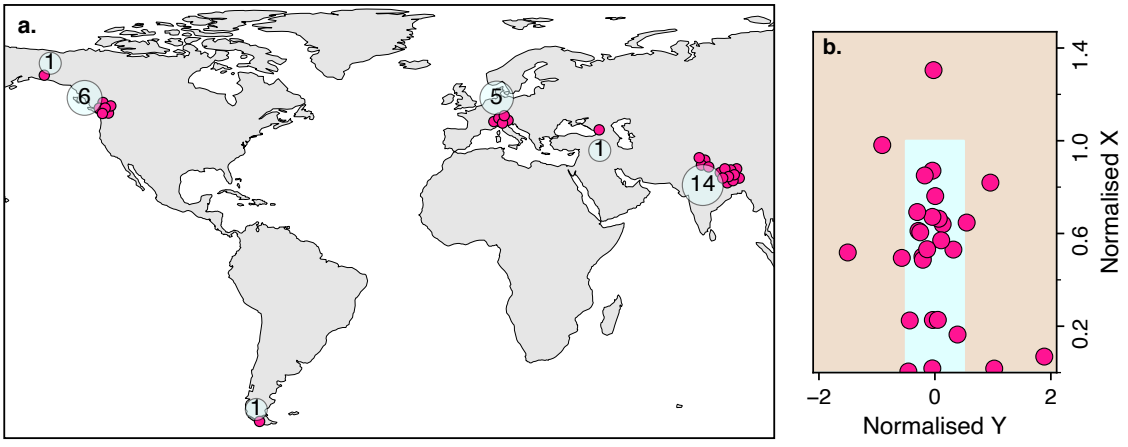

Figure 1. (a) Locations of 28 on- or near-glacier weather stations (red solid circles) used in this study. The circles have been artificially spread out up to about 2° to avoid overlap. The number of stations in different regions are shown within light blue circles. (b) The relative, scaled locations of the weather stations used in this study (red circles) with respect to an idealised glacier (light blue rectangle) having a unit length and width. Here X and Y denotes the longitudinal and transverse distance, respectively.

2.2 Climate and topography

We used ∼9-km resolution ERA5-Land (ERA5L) hourly reanalysis data from European Centre for Medium-Range Weather Forecasts (Hersbach et al., 2020) to obtain the 2-m air temperature, matching the period and location of each of the 28 weather stations. The temperature data were corrected for the station elevation using an hourly lapse rate derived by regressing the temperature and elevation for all the pixels within a 100×100 km^2 buffer centered around the station. The 10-m wind speed from ERA5L was used for comparison with the 2-m windspeed predicted using the model developed here. We did not attempt to correct the ERA5L wind speed to bring it to 2-m level, which was not straightforward as the vertical structure of the boundary layer above glaciers are complex (e.g., Draeger et al., 2024). Glacier geometry data from Randolf Glacier Inventory 7 (RGI7.0-Consortium, 2023) and topographic static variables derived from the 30-m resolution digital elevation model (DEM) from ALOS World 3D (Tadono et al., 2014) was used for predicting the three model parameters (see Sect. 3.1.2).

3 Methods

3.1 Model

3.1.1 Model for wind speed

Empirically, glacier wind is known to have a characteristic diurnal variation, with the maximum wind speed occurring in afternoon (e.g., Obleitner, 1994; Oerlemans et al., 1999; Björnsson et al., 2005). It has also been noted that the timing of the

https://doi.org/10.5194/egusphere-2025-3756
Preprint. Discussion started: 12 September 2025

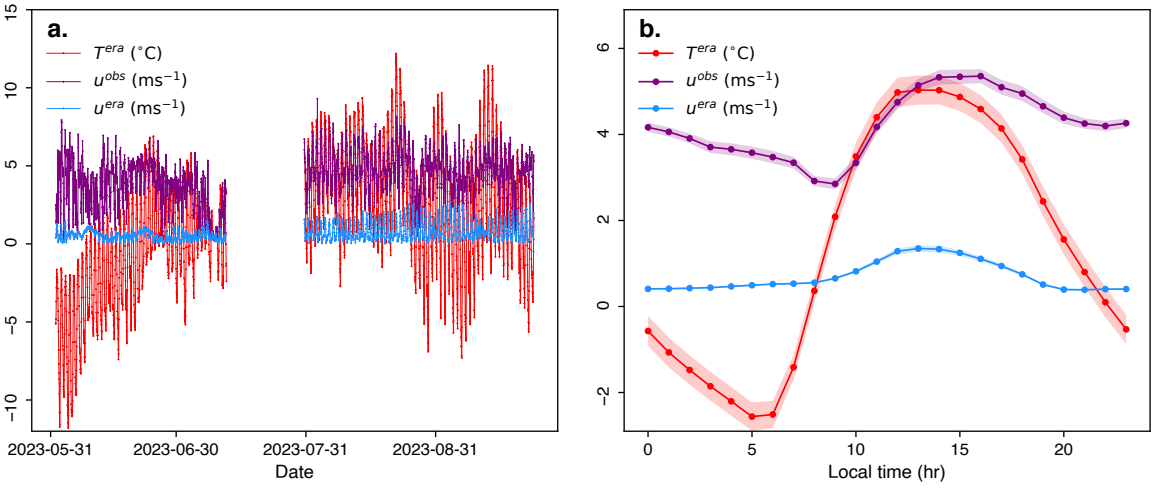

Figure 2. a) Time-series of hourly wind speed (purple line) observed on Drang Drung Glacier in the western Himalaya, along with corresponding ERA5-Land temperature (red line) and wind speed (light blue line) estimates during the summer season of 2023. b) The corresponding mean diurnal cycles, with the standard error of mean shown as shaded bands.

wind speed maxima lags behind that of the temperature by a few hours (Oerlemans and Grisogono, 2002). The time series of the observed wind speed and ERA5-derived temperature for Drang Drung Glacier, the western Himalaya illustrate this behaviour (Fig. 2). It may be seen that the hourly wind-speed signal is noisy (Fig. 2a). However, the mean diurnal wind speed has a smooth variation, which appears to be a delayed response to the mean diurnal 2-m air temperature on this glacier (Fig. 2b). A similar behaviour is known to be present in land-sea breeze and valley-wind systems, and consequently, both of the system could be described well using simple linear-response models (e.g., Nickus and Vergeiner, 1984; Bjerknes, 1898).

Motivated by this, here we attempted to predict the mean diurnal wind speed on or near a glacier, using the corresponding mean diurnal temperature. We restricted our analysis to the summer season as most of the melt happens during this time. Let u denote the mean summertime diurnal wind speed, which was decomposed into its mean value $\bar{u}$ and the diurnal anomaly u_d, i.e., $u \doteq \bar{u} + u_d$. Similarly, the mean summertime diurnal temperature was decomposed into $\bar{T}$ and T_d. Then, we modelled u_d as a linear combination T_d and its time derivative $\frac{d}{dt}T_d$ to obtain the following equation:

$$u = \bar{u} + sT_d - s\tau\frac{d}{dt}T_d, \tag{1}$$

where s is the sensitivity of the mean diurnal wind-speed anomaly to that of temperature, and τ is the corresponding response time. Note that this is not a traditional linear response model (e.g., Boyce et al., 2017; Oerlemans, 2005), where the forcing T_d is taken to be a linear combination of the response u_d and its time derivative $\frac{d}{dt}u_d$. We chose the present version over a traditional linear-response model because the derivative of wind speed was found to be relatively more noisy as compared to

https://doi.org/10.5194/egusphere-2025-3756
Preprint. Discussion started: 12 September 2025

that of temperature (Fig. 2b), which resulted in poor fits. In our problem, the dominant frequency ω was diurnal (~ 0.26 hr^{-1}) and the typical response time τ was a few hours , so that $\omega^2\tau^2 \to 0$. In this limit, both models were in fact equivalent to each other (Supplementary Text S1).

3.1.2 Model parameters

To apply the above model to an ungauged glacier, one requires the knowledge of T_d and three model parameters $\bar{u}$, s, and τ for that location. It is possible to obtain T_d from reanalysis datasets. However, the model parameters are not known a priori. Wind speeds on complex terrain have been linked to topography before (Helbig et al., 2017; Burlando et al., 2007). Motivated by this, we test if the model parameters $\bar{u}$, s, and τ can be estimated for any given glacier as simple linear combinations of static variables associated with glacier geometry and local topography etc., i.e.,

$$\bar{u} = \beta_0^u + \beta_1^u \pi_1^u + \beta_2^u \pi_2^u + \cdots, \tag{2}$$

$$s = \beta_0^s + \beta_1^s \pi_1^s + \beta_2^s \pi_2^s + \cdots, \tag{3}$$

$$\tau = \beta_0^\tau + \beta_1^\tau \pi_1^\tau + \beta_2^\tau \pi_2^\tau + \cdots, \tag{4}$$

where π_i^x denotes the i^{th} static variable, and β_i^x denotes the corresponding regression coefficient for the model parameter x.

We searched through a list of 37 static variables (Supplementary Table S2) to come up with the best set of predictors π_i^x. The static variables included 22 valley/glacier-geometry variables (like width and length of the glacier/valley), 12 topographic variables (like relief and mean elevation), and three climatic variables (e.g., continentality). For deriving the topographic variables for a station location from the DEM, a combination of QGIS (QGIS Development Team, 2024) and Google Earth Engine (GEE) (Gorelick et al., 2017) was used (Supplementary Table S2).

3.2 Calibrating model

3.2.1 Fitting Eq. 1 to observations

The model parameter $\bar{u}$ for each of the 28 stations was obtained by averaging the observed mean summertime diurnal wind speed u^{obs}. The remaining two model parameters s and τ were obtained for each station by performing a bilinear least-square regression of T_d and its derivative $\frac{d}{dt}T_d$, against u_d^{obs} (Eq. 1). This obtained 28 triplets of best-fit parameters $\{\bar{u}, s, \tau\}$ – one each for each station. Here, the diurnal variation T_d was obtained by decomposing the ERA5L-derived mean diurnal summertime temperature T^{era}, into its mean and the anomalies. The time derivative of T_d was obtained by calculating the first differences. The root-mean-squared errors (RMSE) of the fits were used to assess the model performance.

3.2.2 Fitting Eqs. 2–4 to model parameters

The best-fit regression coefficients in Eq. 2 were obtained by regressing the 28 values of $\bar{u}$ against the static variables. While the RMSE of a multilinear regression generally decreases with the increasing number of static variables, we limited the number of static variables used in Eq. 2 by the following method, to avoid over-fitting. For an n-variable regression model, there

https://doi.org/10.5194/egusphere-2025-3756
Preprint. Discussion started: 12 September 2025

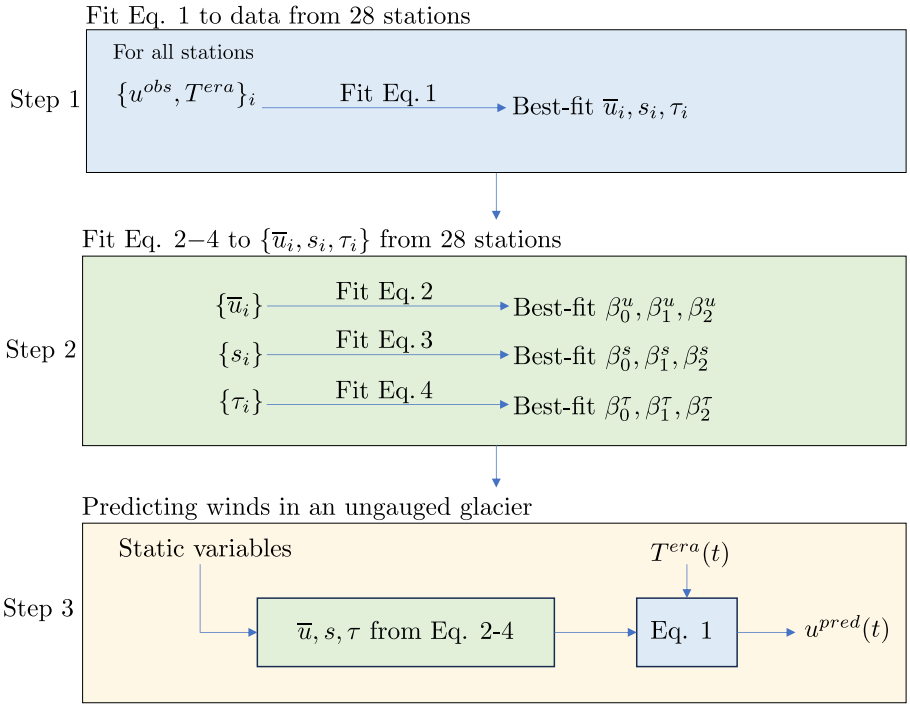

Figure 3. The three-step workflow for modelling the mean summertime diurnal wind on an ungauged glacier. (Step 1) Wind speed and ERA5 temperature in each station were fitted to Eq 1 separately, obtaining 28 triplets of best-fit $\bar{u}, s$, and τ. (Step 2) This set of 28 triplets—excluding s and τ from Langenferner Glacier, as discussed in section 4.1.2—were used to obtain the best-fit multi-linear regression coefficients defined in Eqs. 2–4. (Step 3) For any ungauged glacier location, the best-fit Eqs. 2–4 were used to predict the three model parameters, which along with the ERA5L temperature, were fed to Eq. 1 to obtain the wind speed predictions.

were $\binom{37}{n}$ possible choices for the static variables. For the given n, starting from $n = 1$, all such possible combinations were systematically tested to find the set of static variables having the lowest RMSE between the predicted and observed $\bar{u}$ for the 28 stations. This procedure was repeated for n varying from 1, 2, 3, ... The iteration was stopped when the reduction in RMSE upon adding a new variable ($n \rightarrow n+1$) was smaller than the reduction achieved in the previous step (Supplementary Fig. S2). The same procedure was then repeated to find the best-fit regression coefficients for Eqs. 3, 4, which were used to predict s and τ, respectively, for any glacier.

https://doi.org/10.5194/egusphere-2025-3756
Preprint. Discussion started: 12 September 2025

3.3 Model performance

3.3.1 Performance of the calibrated model

The performance of the model (Eqs. 1–4), which was calibrated using the procedure described above, was tested on each of the 28 weather stations. For each station, the mean summertime diurnal wind speed predicted by the calibrated model at hourly time steps were compared with the corresponding observed values. Note that these predicted values were obtained from the calibrated equations, only using the corresponding ERA5L temperature and the static variables as inputs. The mean, median, and interquartile range of the set of 28 RMSEs between the model predictions and observations were compared with the set of RMSEs between the ERA5L products and observations.

3.3.2 Leave-One-Out-Cross-Validation

To evaluate the performance of the model for an ungauged location, we performed a Leave-One-Out-Cross-Validation (LOOCV) (Hastie et al., 2009). For this, we calibrated the model following the procedure described in Sect. 3.2 with 27 out of 28 weather stations. The calibrated model was then used to predict the wind speed at the 28th weather station, using only the corresponding ERA5L temperature and the static variables, and without using any in-situ data from the 28th station. We repeated this process 28 times, leaving out a different station each time, and computing the RMSE between the predicted and observed wind speeds for the left-out station.

3.3.3 Minimum number of stations required

We tested how sensitive the predictions from the calibrated model were to the number of stations available for calibration. To do this, the model was calibrated only using a randomly selected subset of N stations. The step was repeated for $N = 13, 14, ..., 28$. For each subset, the model was calibrated exactly as discussed in Sect. 3.2, and then evaluated across all 28 stations by computing the RMSEs between the observed and predicted mean summertime diurnal wind speed. The mean RMSE was recorded. The exercise was repeated 100 times to obtain a set of 100 mean RMSEs for each N. The resulting distributions of RMSEs were plotted as a function of N, to see if the RMSEs converge to a fixed value with increasing N. Note that this exercise was also helpful in ascertaining the model performance on ungauged glaciers, as only a subset of glaciers were used here to calibrate the model, which was then used to predict the wind speed on all 28 stations.

3.3.4 Time scale dependence of prediction

We tested if the calibrated model, which was derived for mean summertime diurnal winds, could be used to predict wind speeds across different time scales. We first filtered the ERA5L hourly temperature data over different time scales by taking 1-hr to 10-days moving average. For each station and each averaging window, the filtered temperature data were fed into the calibrated model (Sect. 3.2) to obtain wind-speed predictions for that station and that time scale. The RMSE between the predicted and

https://doi.org/10.5194/egusphere-2025-3756
Preprint. Discussion started: 12 September 2025

observed wind speeds was computed for each station, yielding a set of 28 RMSEs. For this RMSE calculation, the observed hourly wind speed data were also filtered using the same moving-average window.

3.4 Estimation of uncertainty

Assuming the uncertainties in the model parameters and the input temperature T^{era} to be uncorrelated with each other, the standard error of the predicted wind speed u^{pred} (Eq. 1), was estimated as follows (e.g., BIPM et al.):

$$\sigma_u = \sqrt{\sigma_{\bar{u}}^2 + s^2\sigma_T^2 + \left(T_d^{era} - \tau\frac{dT_d^{era}}{dt}\right)^2\sigma_s^2 + s^2\tau^2\sigma_{dT/dt}^2 + \left(s\frac{dT_d^{era}}{dt}\right)^2\sigma_\tau^2}. \quad (5)$$

Here σ_T and $\sigma_{dT/dt}$ denote the standard errors of mean of T^{era} and $\frac{d}{dt}T_d$, respectively. These were estimated directly from the hourly ERA5L temperature time-series and its first difference. For estimating the errors in the model parameters $\bar{u}$, s, and τ, which were computed using Eq. 2–4, we used the following from (BIPM et al.):

$$\sigma_x^2 = \sum_{i=0}^{n}\sum_{j=0}^{n}\beta_i^x\beta_j^x\mathcal{C}_{ij}^x, \quad (6)$$

where, x denotes the specific model parameter, n is the number of static variables used in the multilinear regression (Eqs. 2–4), and $\mathcal{C}_{ij}^x$ denotes the covariance of static predictor variables π_i^x and π_j^x.

4 Results

4.1 Model calibration

4.1.1 Fitting Eq. 1 to observations

Equation 1 accurately captured the mean summertime diurnal wind speed across all the weather stations. The results of fitting Eq. 1 to the observed wind speed on a selected weather station shown in Fig. 4a, b. Across the 28 weather stations, the quality of fits varied (Fig. 4c), and the mean (median) RMSE was 0.24 (0.17) ms^{-1} with an interquartile range of 0.12–0.36 ms^{-1}. In contrast, a direct comparison between the ERA5L wind-speed product with the observed mean summertime diurnal wind yielded a mean (median) RMSE of 1.98 (2.09) ms^{-1}, with an interquartile range of 1.29–2.57 ms^{-1}.

The distribution of best-fit model parameters $\bar{u}, s$, and τ obtained for the 28 stations varied significantly (Supplementary Fig. S2). The best-fit mean wind speed $\bar{u}$ ranged from 0.96–5.12 ms^{-1} with a mean (median) value of 2.71 (2.96) ms^{-1}. The best-fit sensitivity s ranged from 0.0–1.04 $ms^{-1}{}^{\circ}C^{-1}$ with a mean (median) value of 0.26 (0.18) $ms^{-1}{}^{\circ}C^{-1}$. The best-fit response time τ ranged between 0–6.3 hr, with a mean (median) value of 1.23 (0.68) hr.

https://doi.org/10.5194/egusphere-2025-3756
Preprint. Discussion started: 12 September 2025

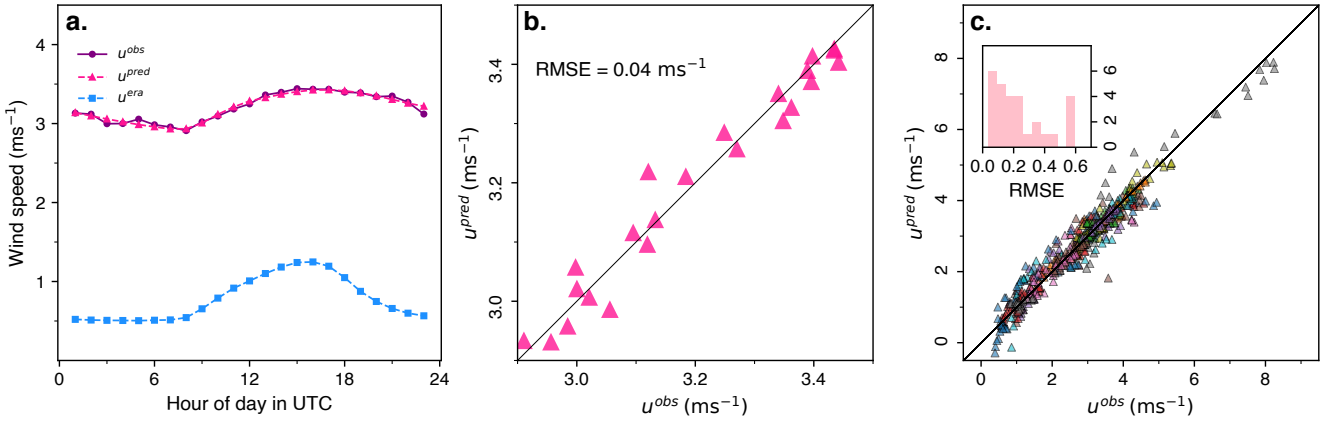

Figure 4. (a) Predicted mean summertime diurnal wind speed (red solid triangle) obtained by fitting Eq. 1 to observations (purple solid circle) for a selected weather station (Place Glacier in British Columbia, see Supplementary table S1). (b) Comparison of the predicted and observed mean wind speeds for this station. (c) Comparison of the predicted and observed mean wind speed for all 28 station, with different symbol colours denoting different stations. The inset shows the distribution of RMSEs obtained in the fits.

4.1.2 Fitting Eqs 2–4 to best-fit model parameters

Following the procedure described in Sect. 3.2.2, the three model parameters $\bar{u}, s$, and τ yielded the following best-fit multi-linear relationships:

$$\bar{u} = (2.5 \pm 0.5) + (0.12 \pm 0.02)AR + (4.5 \pm 0.8) \times 10^{-3} R_1 - (1.5 \pm 0.2) \times 10^{-3} R_5, \quad (7)$$

$$s = (0.13 \pm 0.09) + (2.2 \pm 0.6) \times 10^{-4} \bar{Z}_{10} - (1.7 \pm 0.5) \times 10^{-3} Z_s, \quad (8)$$

$$\tau = (0.73 \pm 0.50) + (1.9 \pm 1.4) S_{0.1}. \quad (9)$$

In the above equations, AR is the ratio of the characteristic transverse and vertical scales of the valley, R_x denotes the x-km relief, $\bar{Z}_x$ denotes the mean elevation within an x-km buffer around the station, Z_s is the elevation of the weather station, and $S_{0.1}$ represents the topographic slope within a 0.1-km buffer around the station (Supplementary Table S2). In calculating the local aspect ratio AR, the vertical scale was defined as the standard deviation of elevation within a 1-km buffer around the station, and the horizontal scale was the width of the valley measured at the station location (see Supplementary Table S2).

The mean wind speed $\bar{u}^{pred}$ predicted using Eq. 7 compared favourably with the corresponding observed values, with a mean RMSE of 0.44 ms^{-1} (Fig. 5b). In comparison, the corresponding mean RMSE for the ERA5L product was 1.88 ms^{-1}, which was 4.2 times higher. In fact, ERA5L products showed a relatively large negative bias, with a mean bias of -1.7 ms^{-1}. Note that while for 27 out of the 28 stations AR <40, Kennikot Glacier is an outlier with AR of 210. This led to an unphysically large mean wind speed ($>$ 24 ms^{-1}) on this glacier while using Eq. 7. This suggests that the linear relationship between AR and $\bar{u}$ breaks down at such large AR. To avoid this issue, we apply an ad-hoc cut-off on the contribution of the second term of Eq. 7 for Kennikot Glacier, corresponding to a value $AR = 40$. Furthermore, winds at Langenferner Glacier was found to

https://doi.org/10.5194/egusphere-2025-3756
Preprint. Discussion started: 12 September 2025

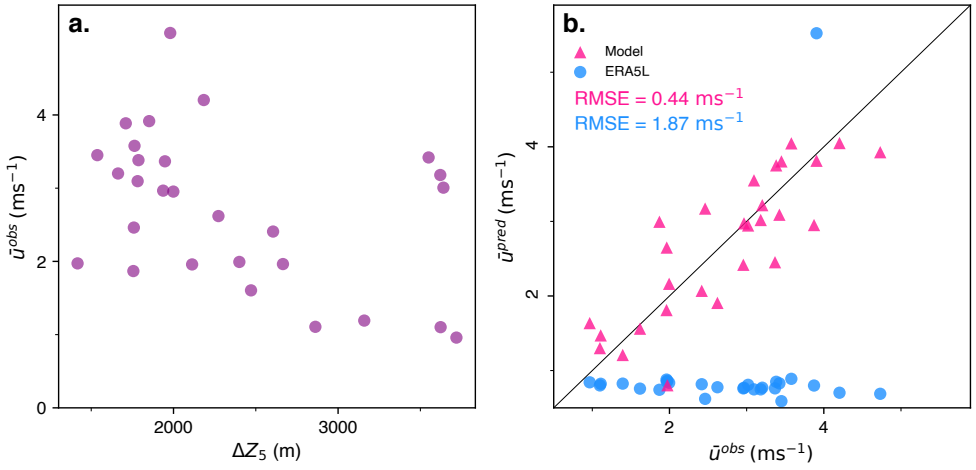

Figure 5. (a) Prediction of mean wind speed using static variables. The model prediction is given as red triangles, and ERA5 wind speed is shown as blue circles. (b) Mean wind speed plotted against most important predictor, 5-km relief. The RMSEs shown are mean values for the 28 stations.

be almost out of phase with temperature (Supplementary Fig. S1), gives rise to unrealistic response times. Therefore, s and τ from this station was left out when fitting Eqs. 3–4 to the 28 triplets of $\{\bar{u}, s, \tau\}$ in section 3.2.

The hourly anomaly of the mean summertime diurnal wind speed predicted using Eqs. 1, 8–9, matched the observations reasonably well with an average RMSE of 0.45 ms^{-1}, although there was some scatter (Fig. 6c). In comparison, ERA5L predicted the diurnal anomaly with an average RMSE of 0.47 ms^{-1}. While these average RMSEs were comparable, the present model prediction captured the diurnal range of wind speed better, which were systematically underestimated by ERA5L (Fig. 6c).

4.2 Model performance

4.2.1 Performance of calibrated model

The calibrated model (Eqs. 1, 7–9) was able to capture the mean summertime diurnal wind speed better than the corresponding ERA5L product for all the weather stations (Fig. 7). For example, the RMSE of the predicted wind speed had a mean (median) value of 0.69 (0.6) ms^{-1}, and an interquartile range of 0.47–0.87 ms^{-1} (Fig. 7). In comparison, the ERA5L wind speed product had about three times higher mean (median) of 1.99 (2.09) ms^{-1}, and a larger interquartile range of 1.29–2.57 ms^{-1}.

4.2.2 Leave-One-Out-Cross-Validation

In general, the result of the LOOCV was satisfactory, and the model fitted to data from 27 stations was able to predict the mean diurnal wind speed at the left-out station reasonably well (Supplementary Fig. S3). In comparison to ERA5L, the set of

https://doi.org/10.5194/egusphere-2025-3756
Preprint. Discussion started: 12 September 2025

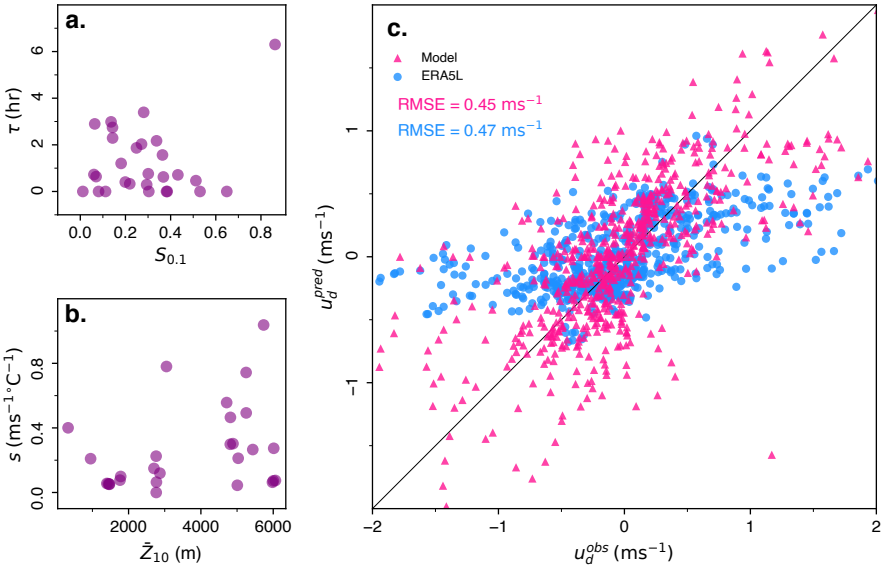

Figure 6. (a-b)The best-fit parameters sensitivity s and response time τ are plotted against their most important static predictors, namely, mean elevation within a 10-km buffer ($\bar{Z}_{10}$), and surface slope within a 0.1-km buffer ($S_{0.1}$). (c) A comparison of the hourly diurnal wind speed anomaly u_d predicted using the model (red solid triangles) and that from the observations. The corresponding comparison for the ERA5L products are also shown (blue solid circles).

28 RMSEs of the wind-speed predicted for the left-out station by the corresponding calibrated model had about 3 times lower mean (0.76 ms^{-1}), median (0.65 ms^{-1}), and interquartile range (0.52–1.01 ms^{-1}).

4.2.3 Minimum number of stations

As long as the number of weather stations available for calibration N was 20 or more, the predictions of the calibrated model remained relatively unaffected (Fig. 8). For example, the mean RMSE for the predictions over all the 28 stations was 0.77 ms^{-1} for $N = 20$, which was within 13% of the mean RMSE value of 0.69 ms^{-1} obtained when all $N = 28$ stations were used for calibration.

4.2.4 Time scales of prediction

While the calibrated model performed better than ERA5L wind speed product across all time-scales, its performance reduced at finer time-resolutions. For moving-average windows of length greater than 96 hr (3 days), the distribution of RMSEs between observed and predicted winds across the 28 stations had a mean value below 1 ms^{-1}. For shorter time-averaging lengths, the

https://doi.org/10.5194/egusphere-2025-3756
Preprint. Discussion started: 12 September 2025

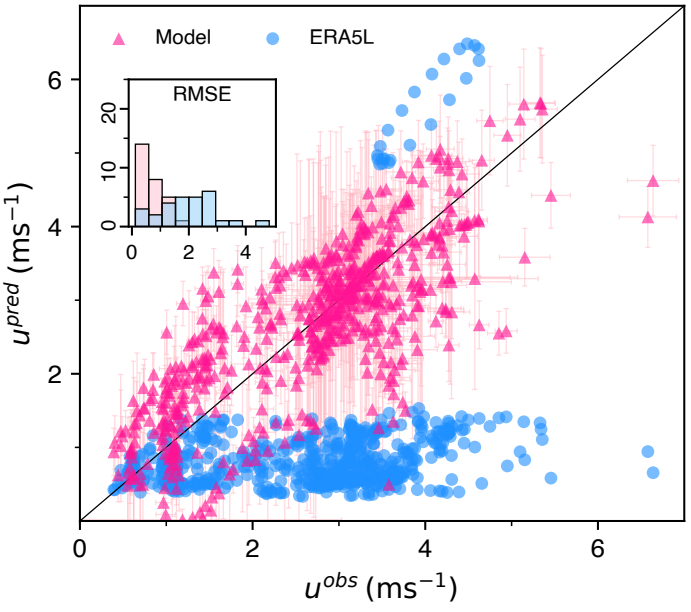

Figure 7. (a) The mean summertime diurnal wind speed predicted using Eqs. 1, 7–9 (red solid triangle) were compared with corresponding observation. The corresponding comparison for ERA5L wind speed are also shown (blue solid circles). The inset shows the distribution of RMSEs for 28 stations for both our model (shown as light pink histogram) and ERA5 (shown as light blue histogram).

mean RMSE increased systemically, with RMSE of ~ 1.7 ms^{-1} for hourly predictions. In comparison, the ERA5L wind speed product had a mean RMSE of more than 2 ms^{-1} across all the time-averaging lengths.

5 Discussion

5.1 Predicting wind speed on ungauged glacier

The proposed model for the mean summertime diurnal wind speed (Eq. 1), which computed the local wind speed on/around glaciers with ERA5L temperature, worked reasonably well for all the 28 weather stations. This may not be unexpected given the existing studies, where thermally driven wind systems such as land-sea breezes and valley-wind circulation have been successfully described as a linear response to diurnal pressure-gradient forcing (e.g., Nickus and Vergeiner, 1984; Vergeiner and Dreiseitl, 1987; Bjerknes, 1898).

The novel result in this study is that the three associated model parameters $\bar{u}, s$, and τ could be predicted for any given glacier using the calibrated multilinear Eqs. 7–9, without the need for any in-situ data. Compared to the wind-speed predicted

https://doi.org/10.5194/egusphere-2025-3756
Preprint. Discussion started: 12 September 2025

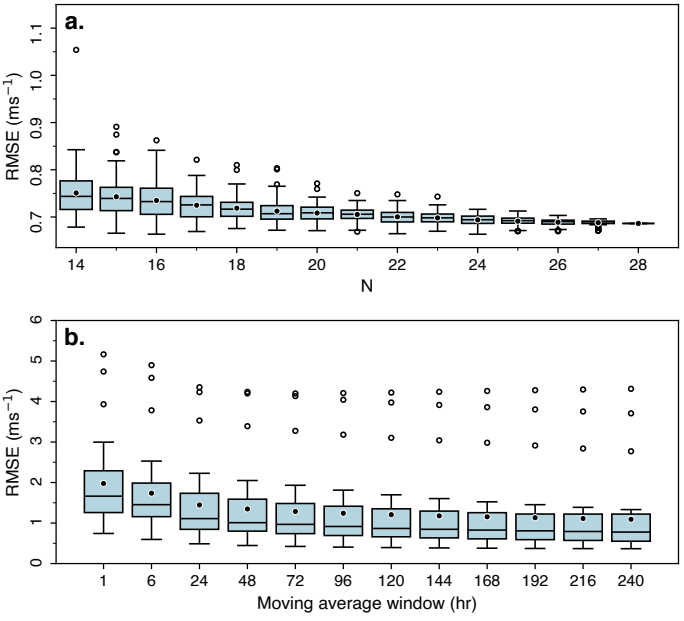

Figure 8. The distribution of RMSEs between predicted and observed wind speed for a) different number of stations N used to calibrate the model, and b) different time-averaging windows. The mean (solid black circle), median (horizontal black line), and outliers (open black circles) of the distributions are shown.

265 directly from the best-fit Eq 1 (Sect. 4.1.1), the wind-speed predicted using the model parameters obtained from the static variable (Eqs. 7–9) were found to be reasonably accurate (Sect. 4.2.1). It is apparent from the LOOCV analysis (Sect. 4.2.2) and the performance of the models calibrated with a smaller subset of stations (Sect. 4.2.3), that the improved performance the present model on ungauged glaciers, as compared to the corresponding ERA5L reanalysis wind-speed products is quite robust. The present model, thus, appears to be a reliable and numerically-efficient alternative to the presently available methods and 270 products, which can be used for estimating local wind speed on ungauged glaciers.

Interestingly, the model appears to perform quite well for the 13 stations that are located near a glacier, and not on it. In addition, it works well for 11 stations located on/near debris-covered glaciers (Supplementary Fig. S1). In all these 16 cases, the station locations are likely to be dominated by valley winds, and not by glacier winds (Supplementary Fig. S1). This suggests that both valley and glacier winds are captured by the same model to a good approximation. Also, it appears that model, which 275 is calibrated for the mean diurnal wind speed over the entire summer season, is still useful at other times scales as well (Sect. 4.2.4). This is because the variability of the mean diurnal wind speed averaged over several days is less than that of the mean wind speed between glaciers (Fig. 5b).

https://doi.org/10.5194/egusphere-2025-3756
Preprint. Discussion started: 12 September 2025

5.2 Predictability of model parameters

As discussed above that the strength of the present model, which predicts the mean summertime diurnal wind speed on any glacier with only ERA5L temperature as input, is that the model parameters are known function (Eqs. 7–9) of a set of easy-to-access static topographic variables. For example, the mean wind speed could be predicted entirely based on the local relief and the aspect ratio of the valley cross-section. This may imply that in general, the local wind speed on glacierised valleys is strongly controlled by the local topography. In particular, the mean wind speed $\bar{u}$ had strong correlation with local relief (Fig. 5a). In comparison, the predictability of the other two model parameters s and τ was relatively low (Fig. 6a, b). In fact, most of the improvements in wind-speed predicted by the present model, over that obtained from ERA5L, was due to the ability of the present model to capture the variability of the mean wind speed $\bar{u}$ between stations (Sect 4.1.2).

While the best multi-linear regressions to obtain the model parameters were found to be Eqs. 7–9 following the methods discussed in Sect 3.2, there were other multilinear regressions that showed similar performance. See Supplementary Sect. S2 for the two next-best models, which had RMSE values within 1% of that obtained in Eqs 5–7. Although these two multilinear regressions involved different static variables, they were similar in nature in that they were alternative definitions of various aspect ratios, relief metrics, and slope.

5.3 Implication for melt calculations

For a rough estimate of the effects of improved estimates of surface wind speed on ice melt calculations, we used a simple bulk-aerodynamic formulation (e.g., Cuffey and Paterson, 2010) to compute the sensible (Q_{shf}) and latent (Q_{lhf}) heat fluxes at all the 28 stations as follows:

$$Q_{shf} = 0.0129\, C^* P\, \bar{u}\, T, \tag{10}$$

$$Q_{lhf} = 22.2\, C^*\, \bar{u}\, (e - e_s). \tag{11}$$

Here, $C^* = 0.002$ is a transfer coefficient (Cuffey and Paterson, 2010), P is the air pressure (in Pa), T is the air temperature (in °C), e is the vapour pressure (in Pa) above the melting surface, and e_s is the vapour pressure (in Pa) at the melting ice surface. The variables P and T were obtained from ERA5. The saturation vapour pressure e_s and actual vapour pressure e were derived from the dew-point temperature obtained from ERA5L (Bolton, 1980; Buck, 1981). The sum of Q_{shf} and Q_{lhf} gave the total turbulent heat flux Q_{thf}. At each station, the turbulent heat flux calculations were repeated thrice for the different estimates of the mean wind speed $\bar{u}$, namely, a) the observed ones, b) those predicted using Eq. 7, and c) those obtained directly from ERA5L.

The mean RMSE between the heat fluxes calculated using the observed wind speed ($\bar{u}^{obs}$) and that predicted using Eq. 7 ($\bar{u}^{pred}$) was 2.2 Wm^{-2} (Fig. 9), which was about 4 times smaller than the mean RMSE of 9.8 Wm^{-2} obtained for the ERA5L derived mean wind speed ($\bar{u}^{era}$). For 17 out of the total 28 stations, where the net Q_{thf} was positive, the heat fluxes increased by a factor of 3.4 on average. For the remaining 11 stations with net negative turbulent heat fluxes, the magnitude of the fluxes increased by a factor of 3.2. This suggested that the turbulent heat fluxes on glaciers might be systematically underestimated

https://doi.org/10.5194/egusphere-2025-3756
Preprint. Discussion started: 12 September 2025

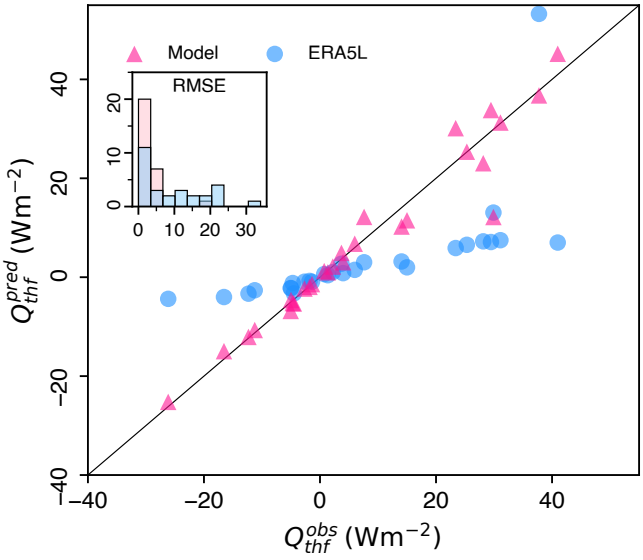

Figure 9. Total turbulent heat flux Q_{thf}^{pred} derived using the mean wind speed predicted in this study (red triangles), and those from ERA5L (blue circles) are compared with the turbulent heat flux Q_{thf}^{obs} computed using observed wind speed. Inset shows the corresponding distributions of RMSEs for the 28 stations.

when ERA5L wind-speed products are used. This is due to a general underestimation of surface-wind speed by ERA5L at the stations (Fig. 5b). While Eq. 7 captures the variability of wind speed between stations, that does not necessarily ensure the corresponding estimates Q_{thf}^{pred} reproduce well the variability of the total turbulent heat fluxes between the stations at a global scale. This is because the temperature and humidity dependent factors in Eq. 10,11 can potentially vary strongly between regions. However, for a given region, the spatial variability of turbulent heat flux is likely to be controlled mainly by that of the wind speed. Therefore, the present model can help in improving the turbulent heat flux calculations for a region significantly, compared to that done using ERA5L-derived wind speed. This is also evident from the 4 times lower mean RMSE between heat fluxes calculated using the model and that using ERA5L-derived winds. It should also be noted that the values of turbulent heat fluxes estimated using the bulk aerodynamic method are meant to be illustrative in nature. Although such methods have been used widely and shown to outperform profile-based methods when a wind speed maximum is present (Denby and Greuell, 2000), recent reports suggest they may perform poorly on glaciers where their underlying assumptions may be unrealistic (Litt et al., 2015; Radić et al., 2017; Steiner et al., 2018).

5.4 Limitations

We acknowledge that the present model provides only a first-order solution to the problem of estimating the surface winds on or near a glacier. First of all, the present results pertain to the mean summertime diurnal wind, while the wind speed is expected to vary over different timescales – hourly, daily,and weekly, (e.g., Fig. 2a) to seasonal and annual. However, our analysis over

https://doi.org/10.5194/egusphere-2025-3756
Preprint. Discussion started: 12 September 2025

different time windows (Sect. 4.2.4) suggests that the magnitude of such temporal variability over time scales of weeks or longer is often not very large compared to the variability of the mean winds between stations.

An interannual variation of the mean summertime wind speed was apparent at the stations with more than one year of data (Supplementary Fig. S5). Such a temporal variability is, of course, not captured by the present model, which produces a time-independent prediction for mean winds at each station based on Eq. 6. For example, the mean value of the fractional absolute interannual deviation was less than 10% in all but two of the studied locations (Supplementary Fig. S5), suggesting that the mean wind speed predicted using Eq. 7 are still useful. More work is needed, possibly utilising a larger set of stations with longer records, to see if the observed temporal variability could be incorporated into the present model with the help of additional time-dependent meteorological variables.

Another related issue with the present model is that the improved predictions of the mean wind speed are entirely based on a few static topographic variables. This implies that it does not capture the climate response of the wind speed. Given that the glacier wind speed is expected to have some temperature response at different time scales (Thangprasert and Suwanarat, 2017, ; also see Fig. 1a), more work is needed to incorporate the effects of climate change in Eq. 7.

A significant spatial variability of the surface wind within any given glacierised valley is expected (e.g., Cai et al., 2007), which may not be captured fully by the present model. Also, in glacierised valleys, there is a competition between the valley and the glacier winds at the surface level, which flow in opposite directions during the daytime. The present formulation is likely to fail over the region near the glacier terminus where these two winds collide. In fact, the present model gives only wind speed and not the wind direction.

There were some peculiarities in the mean summertime diurnal wind speed at a few stations, which could not be captured by the present model. For example, some stations there were additional early-morning maxima of wind speed (Supplementary Fig. S1), apart from the prominent late-afternoon one. This behaviour could not be reproduced with the present temperature-based linear response model, as the mean diurnal temperature decreased monotonically between sunset and sunrise. At Langenferner Glacier, the temperature and wind speed was out of phase (Supplementary Fig. S1), which was unusual. Here Eq. 1 could not be fitted to the data for a finite τ, and the wind-speed predictions using Eqs. 1, 7–9 produced a large RMSE (Supplementary Table S4).

Most of the improvement in mean summertime diurnal wind speed predicted using the present model, vis-a-vis the estimates obtained directly from ERA5L, was due to a better estimation of the mean wind speed $\bar{u}^{pred}$ by the former. As discussed above, the mean RMSEs for $\bar{u}^{pred}$ was 4.2 times smaller in the present model, compared to that of the corresponding ERA5L product. In addition, the ERA5L had a significant negative bias, which was 1.9 ms^{-1} on average, for $\bar{u}$. In contrast, both the present model and ERA5L had similar mean RMSEs for the diurnal anomaly u_d, indicating that there is scope for improving the estimates of the model parameters s and τ.

https://doi.org/10.5194/egusphere-2025-3756
Preprint. Discussion started: 12 September 2025

6 Conclusion

In this study, we propose a model to estimate the mean summertime diurnal wind speed on any ungauged glacier. Given the values of three model parameters, the model obtains the wind speed as a linear combination of the mean summertime diurnal temperature and its time derivative. The required input temperature data are derived from a reanalysis product (ERA5-Land). We show that this model captures well the observed mean summer diurnal wind speed on 28 on- or near-glacier weather stations across the globe. Interestingly, an analysis of the 28 triplets of best-fit model parameters—excluding s and τ from Langenferner Glacier, as discussed in section 4.1.2—established that the parameters can be approximated as multilinear functions of a few static topographic variables. This implies that the present model can be applied to ungauged glaciers, which is encouraging. A leave-one-out-cross-validation indicated that the method indeed works reasonably on ungauged glaciers, and may improve the RMSE between the observed and estimated mean summertime diurnal wind speeds by about 300% on average, compared to the corresponding reanalysis estimates. Most of this improvement is, in fact, due to the ability of the present model to capture the variability of the mean summertime wind between glaciers better than the reanalysis product. The number of stations used for calibrating the model is shown to be adequate for robust predictions. We discuss the limitations of the model in capturing the temporal variability of wind speed over different time scales. Using this model to parameterise the mean summertime diurnal wind speed may improve the turbulent heat flux estimates on glacierised valleys, which tend to be underestimated with reanalysis wind speed products. Understanding the physical basis of the predictability of the mean summertime wind speed on valley glaciers based on a set of topographic parameters, and improving the estimates of the other two model parameters emerge as two of the most interesting open problems.

Code and data availability. The github repository https://github.com/krrishj2000/Mountain_glacier_winds_parameterisation contains all codes and processed data used in this work.

Author contributions. KJ and AB designed the study, conceived the model, and wrote the paper. KJ compiled the meteorological data, did the data analysis, and prepared the figures. RS contributed to the theoretical development. HK and MFA provided field data from Drang Drung Glacier. All authors participated in the discussions, and edited the manuscript.

Competing interests. Authors declare no competing interests.

Acknowledgements. We thank Joseph Shea for sharing weather station data from Place and Weart Glaciers. We acknowledge the contribution of H C Nainwal and his team to the field measurements on Satopanth Glacier. We thank the Ev-K2-CNR Committee for making the data from the weather stations around Khumbu Glacier available. We also thank the two anonymous reviewers of the previous version of the manuscript

https://doi.org/10.5194/egusphere-2025-3756
Preprint. Discussion started: 12 September 2025

for their constructive comments. KJ is supported by INSPIRE scholarship from the Department of Science and Technology, Government of India.

https://doi.org/10.5194/egusphere-2025-3756
Preprint. Discussion started: 12 September 2025

References

Arndt, A., Scherer, D., and Schneider, C.: Atmosphere Driven Mass-Balance Sensitivity of Halji Glacier, Himalayas, Atmosphere, 12, https://doi.org/10.3390/atmos12040426, 2021.

Ayala, A., Pellicciotti, F., and Shea, J. M.: Modeling 2-m air temperatures over mountain glaciers: Exploring the influence of katabatic cooling and external warming, Journal of Geophysical Research: Atmospheres, 120, 3139–3157, https://doi.org/https://doi.org/10.1002/2015JD023137, 2015.

Azam, M. F., Wagnon, P., Vincent, C., Ramanathan, A., Favier, V., Mandal, A., and Pottakkal, J. G.: Processes governing the mass balance of Chhota Shigri Glacier (western Himalaya, India) assessed by point-scale surface energy balance measurements, The Cryosphere, 8, 2195–2217, https://doi.org/10.5194/tc-8-2195-2014, 2014.

BIPM, IEC, IFCC, ILAC, ISO, IUPAC, IUPAP, and OIML: Evaluation of measurement data — Guide to the expression of uncertainty in measurement, Joint Committee for Guides in Metrology, JCGM 100:2008, https://doi.org/https://doi.org/10.59161/JCGM100-2008E.

Bjerknes, V.: Ueber einen Hydrodynamischen Fundamentalsatz und seine Anwendung: besonders auf die Mechanik der Atmosphäre und des Weltmeeres, Handlingar, K. Svenska Vetenskaps-Akademiens, Kungl. Boktryckeriet. P. A. Norstedt & Söner, https://books.google.co.in/books?id=JQL8GwAACAAJ, 1898.

Björnsson, H., Gudmundsson, S., and Pálsson, F.: Glacier winds on Vatnajökull ice cap, Iceland, and their relation to temperatures of its lowland environs, Annals of Glaciology, 42, 291–296, https://doi.org/10.3189/172756405781812493, 2005.

Bolton, D.: The Computation of Equivalent Potential Temperature, Monthly Weather Review, 108, 1046 – 1053, https://doi.org/10.1175/1520-0493(1980)108<1046:TCOEPT>2.0.CO;2, 1980.

Boyce, W. E., DiPrima, R. C., and Meade, D. B.: Elementary differential equations, John Wiley & Sons, 2017.

Broeke, V. D.: Momentum, Heat, and Moisture Budgets of the Katabatic Wind Layer over a Midlatitude Glacier in Summer, Journal of Applied Meteorology, 36, 763 – 774, https://doi.org/10.1175/1520-0450(1997)036<0763:MHAMBO>2.0.CO;2, 1997a.

Broeke, V. D.: Structure and diurnal variation of the atmospheric boundary layer over a mid-latitude glacier in summer, Boundary-Layer Meteorology, 83, 183–205, 1997b.

Buck, A. L.: New Equations for Computing Vapor Pressure and Enhancement Factor, Journal of Applied Meteorology and Climatology, 20, 1527 – 1532, https://doi.org/10.1175/1520-0450(1981)020<1527:NEFCVP>2.0.CO;2, 1981.

Burlando, M., Carassale, L., Georgieva, E., Ratto, C. F., and Solari, G.: A simple and efficient procedure for the numerical simulation of wind fields in complex terrain, Boundary-layer meteorology, 125, 417–439, 2007.

Cai, X., Song, Y., Zhu, T., Lin, W., and Kang, L.: Glacier winds in the Rongbuk Valley, north of Mount Everest: 2. Their role in vertical exchange processes, Journal of Geophysical Research: Atmospheres, 112, https://doi.org/https://doi.org/10.1029/2006JD007868, 2007.

Collier, E., Maussion, F., Nicholson, L. I., Mölg, T., Immerzeel, W. W., and Bush, A. B. G.: Impact of debris cover on glacier ablation and atmosphere–glacier feedbacks in the Karakoram, The Cryosphere, 9, 1617–1632, https://doi.org/10.5194/tc-9-1617-2015, 2015.

Cuffey, K. and Paterson, W.: The Physics of Glaciers, Academic Press, ISBN 9780080919126, https://books.google.co.in/books?id=Jca2v1u1EKEC, 2010.

Denby, B. and Greuell, W.: The use of bulk and profile methods for determining surface heat fluxes in the presence of glacier winds, Journal of Glaciology, 46, 445–452, https://doi.org/10.3189/172756500781833124, 2000.

Draeger, C., Radić, V., White, R. H., and Tessema, M. A.: Evaluation of reanalysis data and dynamical downscaling for surface energy balance modeling at mountain glaciers in western Canada, The Cryosphere, 18, 17–42, 2024.

https://doi.org/10.5194/egusphere-2025-3756
Preprint. Discussion started: 12 September 2025

Dujardin, J. and Lehning, M.: Wind-Topo: Downscaling near-surface wind fields to high-resolution topography in highly complex terrain with deep learning, Quarterly Journal of the Royal Meteorological Society, 148, 1368–1388, https://doi.org/https://doi.org/10.1002/qj.4265, 2022.

Farina, S. and Zardi, D.: Understanding thermally driven slope winds: recent advances and open questions, Boundary-Layer Meteorology, 189, 5–52, 2023.

Goger, B., Stiperski, I., Nicholson, L., and Sauter, T.: Large-eddy simulations of the atmospheric boundary layer over an Alpine glacier: Impact of synoptic flow direction and governing processes, Quarterly Journal of the Royal Meteorological Society, 148, 1319–1343, https://doi.org/https://doi.org/10.1002/qj.4263, 2022.

Gorelick, N., Hancher, M., Dixon, M., Ilyushchenko, S., Thau, D., and Moore, R.: Google Earth Engine: Planetary-scale geospatial analysis for everyone, Remote Sensing of Environment, https://doi.org/10.1016/j.rse.2017.06.031, 2017.

Greuell, W. and Böhm, R.: 2 m temperatures along melting mid-latitude glaciers, and implications for the sensitivity of the mass balance to variations in temperature, Journal of Glaciology, 44, 9–20, https://doi.org/10.3189/S0022143000002306, 1998.

Hastie, T., Tibshirani, R., Friedman, J. H., and Friedman, J. H.: The elements of statistical learning: data mining, inference, and prediction, vol. 2, Springer, 2009.

Helbig, N., Mott, R., van Herwijnen, A., Winstral, A., and Jonas, T.: Parameterizing surface wind speed over complex topography, Journal of Geophysical Research: Atmospheres, 122, 651–667, https://doi.org/https://doi.org/10.1002/2016JD025593, 2017.

Hersbach, H., Bell, B., Berrisford, P., Hirahara, S., Horányi, A., Muñoz-Sabater, J., Nicolas, J., Peubey, C., Radu, R., Schepers, D., Simmons, A., Soci, C., Abdalla, S., Abellan, X., Balsamo, G., Bechtold, P., Biavati, G., Bidlot, J., Bonavita, M., De Chiara, G., Dahlgren, P., Dee, D., Diamantakis, M., Dragani, R., Flemming, J., Forbes, R., Fuentes, M., Geer, A., Haimberger, L., Healy, S., Hogan, R. J., Hólm, E., Janisková, M., Keeley, S., Laloyaux, P., Lopez, P., Lupu, C., Radnoti, G., de Rosnay, P., Rozum, I., Vamborg, F., Villaume, S., and Thépaut, J.-N.: The ERA5 global reanalysis, Quarterly Journal of the Royal Meteorological Society, 146, 1999–2049, https://doi.org/https://doi.org/10.1002/qj.3803, 2020.

Hock, R.: A distributed temperature-index ice- and snowmelt model including potential direct solar radiation, Journal of Glaciology, 45, 101–111, https://doi.org/10.3189/S0022143000003087, 1999.

Hock, R.: Temperature index melt modelling in mountain areas, Journal of Hydrology, 282, 104–115, https://doi.org/https://doi.org/10.1016/S0022-1694(03)00257-9, mountain Hydrology and Water Resources, 2003.

Hu, W., Scholz, Y., Yeligeti, M., Bremen, L. v., and Deng, Y.: Downscaling ERA5 wind speed data: a machine learning approach considering topographic influences, Environmental Research Letters, 18, 094 007, https://doi.org/10.1088/1748-9326/aceb0a, 2023.

Klok, E., Nolan, M., and Van den Broeke, M.: Analysis of meteorological data and the surface energy balance of McCall Glacier, Alaska, USA, Journal of Glaciology, 51, 451–461, 2005.

Kronenberg, M., van Pelt, W., Machguth, H., Fiddes, J., Hoelzle, M., and Pertziger, F.: Long-term firn and mass balance modelling for Abramov Glacier in the data-scarce Pamir Alay, The Cryosphere, 16, 5001–5022, 2022.

Lin, C., Yang, K., Chen, D., Guyennon, N., Balestrini, R., Yang, X., Acharya, S., Ou, T., Yao, T., Tartari, G., and Salerno, F.: Summer afternoon precipitation associated with wind convergence near the Himalayan glacier fronts, Atmospheric Research, 259, 105 658, https://doi.org/https://doi.org/10.1016/j.atmosres.2021.105658, 2021.

Litt, M., Sicart, J.-E., Helgason, W. D., and Wagnon, P.: Turbulence characteristics in the atmospheric surface layer for different wind regimes over the tropical Zongo glacier (Bolivia, 16○ S), Boundary-layer meteorology, 154, 471–495, 2015.

https://doi.org/10.5194/egusphere-2025-3756
Preprint. Discussion started: 12 September 2025

Mandal, A., Angchuk, T., Azam, M. F., Ramanathan, A., Wagnon, P., Soheb, M., and Singh, C.: An 11-year record of wintertime snow-surface energy balance and sublimation at 4863 m asl on the Chhota Shigri Glacier moraine (western Himalaya, India), The Cryosphere, 16, 3775–3799, 2022.

Mannouji, N.: A numerical experiment on the mountain and valley winds, Journal of the Meteorological Society of Japan. Ser. II, 60, 1085–1105, 1982.

Miller, S., Keim, B., Talbot, R., and Mao, H.: Sea breeze: Structure, forecasting, and impacts, Reviews of Geophysics - REV GEOPHYS, 41, https://doi.org/10.1029/2003RG000124, 2003.

Nickus, U. and Vergeiner, I.: The thermal structure of the Inn Valley atmosphere, Archives for meteorology, geophysics, and bioclimatology, Series A, 33, 199–215, 1984.

Obleitner, F.: Climatological features of glacier and valley winds at the Hintereisferner (Ötztal Alps, Austria), Theoretical and Applied Climatology, 49, 225–239, 1994.

Oerlemans and Grisogono: Glacier winds and parameterisation of the related surface heat fluxes, Tellus A: Dynamic Meteorology and Oceanography, 54, 440–452, https://doi.org/10.3402/tellusa.v54i5.12164, 2002.

Oerlemans, Björnsson, H., Kuhn, M., Obleitner, F., Palsson, F., Smeets, C., Vugts, H., and Wolde, J. D.: Glacio-meteorological investigations on Vatnajökull, Iceland, summer 1996: An overview, Boundary-layer meteorology, 92, 3–24, 1999.

Oerlemans, J.: Glaciers and climate change, CRC Press, 2001.

Oerlemans, J.: Extracting a Climate Signal from 169 Glacier Records, Science, 308, 675–677, https://doi.org/10.1126/science.1107046, 2005.

Oerlemans, J.: The microclimate of valley glaciers, IGITUR, Universiteitsbibliotheek Utrecht, ISBN 987-90-393-5305-5, 2010.

Prandtl, L.: Essentials of Fluid Dynamics: With Applications to Hydraulics, Aeronautics, Meteorology and Other Subjects., 1952.

QGIS Development Team: QGIS Geographic Information System, Open Source Geospatial Foundation Project, http://qgis.osgeo.org, 2024.

Radić, V., Menounos, B., Shea, J., Fitzpatrick, N., Tessema, M. A., and Déry, S. J.: Evaluation of different methods to model near-surface turbulent fluxes for a mountain glacier in the Cariboo Mountains, BC, Canada, The Cryosphere, 11, 2897–2918, https://doi.org/10.5194/tc-11-2897-2017, 2017.

RGI7.0-Consortium: Randolph Glacier Inventory - A Dataset of Global Glacier Outlines, Version 7.0, https://doi.org/10.5067/f6jmovy5navz, 2023.

Rupper, S. and Roe, G.: Glacier Changes and Regional Climate: A Mass and Energy Balance Approach, Journal of Climate, 21, 5384 – 5401, https://doi.org/10.1175/2008JCLI2219.1, 2008.

Rye, C. J., Arnold, N. S., Willis, I. C., and Kohler, J.: Modeling the surface mass balance of a high Arctic glacier using the ERA-40 reanalysis, Journal of Geophysical Research: Earth Surface, 115, 2010.

Shea, J. M. and Moore, R. D.: Prediction of spatially distributed regional-scale fields of air temperature and vapor pressure over mountain glaciers, Journal of Geophysical Research: Atmospheres, 115, https://doi.org/https://doi.org/10.1029/2010JD014351, 2010.

Steiner, J. F., Litt, M., Stigter, E. E., Shea, J., Bierkens, M. F., and Immerzeel, W. W.: The importance of turbulent fluxes in the surface energy balance of a debris-covered glacier in the Himalayas, Frontiers in Earth Science, 6, 144, 2018.

Stigter, E. E., Litt, M., Steiner, J. F., Bonekamp, P. N. J., Shea, J. M., Bierkens, M. F. P., and Immerzeel, W. W.: The Importance of Snow Sublimation on a Himalayan Glacier, Frontiers in Earth Science, Volume 6 - 2018, https://doi.org/10.3389/feart.2018.00108, 2018.

https://doi.org/10.5194/egusphere-2025-3756
Preprint. Discussion started: 12 September 2025

Tadono, T., Ishida, H., Oda, F., Naito, S., Minakawa, K., and Iwamoto, H.: Precise Global DEM Generation by ALOS PRISM, ISPRS Annals of the Photogrammetry, Remote Sensing and Spatial Information Sciences, II-4, 71–76, https://doi.org/10.5194/isprsannals-II-4-71-2014, 2014.

Thangprasert, N. and Suwanarat, S.: The Relationships between Wind Speed and Temperature Time Series in Bangkok, Thailand., in: Journal of physics: conference series, vol. 901, p. 012043, IOP Publishing, 2017.

Tiwari, U. and Bush, A. B. G.: Understanding the Atmospheric Dynamics over High-Altitude Glaciated Regions in the Central Himalayas Using High-Resolution Numerical Simulations, Journal of Hydrometeorology, 26, 239 – 257, https://doi.org/10.1175/JHM-D-24-0084.1, 2025.

Vergeiner, I. and Dreiseitl, E.: Valley winds and slope winds — Observations and elementary thoughts, Meteorology and Atmospheric Physics, 36, 264–286, https://doi.org/10.1007/BF01045154, 1987.

Yáñez San Francisco, E., MacDonell, S., and Casassa, G.: The Importance of a Glacier Complex for Downstream Runoff in the Semiarid Chilean Andes During Dry Years, Hydrological Processes, 39, e70 064, https://doi.org/https://doi.org/10.1002/hyp.70064, e70064 HYP-24-0526.R1, 2025.